文章编号：1001－9014(2017)03－0266－05

DOI:10.11972/j.issn.1001－9014.2017.03.003

Influence of wavelength of probe laser on terahertz free-space electro-optic sampling detection

DU Hai-Wei*, PENG Xiao-Yu

(Center for Terahertz Technology Research, Chongqing Institute of Green and Intelligent Technology, Chinese Academy of Sciences, Chongqing 400714, China)

Abstract: The wavelength of the probe laser can affect the bandwidth and the efficiency of terahertz electro-optic sampling (EOS) detection method because of the relationship of velocity match between the terahertz phase velocity and the laser group velocity. An electro-optic (EO) crystal has different dispersion with different lasers, thus the wavelength of the probe laser for a given EO crystals have different influence on the EOS detection. The response functions of EOS systems based on two typical EO crystals, ZnTe and GaP, have been studied. The results show that the probe laser with wavelengths of 800 nm and 1200 nm are more suitable for the ZnTe- and GaP-based EOS system, respectively, than other selected wavelengths (600 nm, 800 nm, 1200 nm and 1600 nm). We also found that for a given thickness of an EO crystal, there exists an optimal wavelength for the probe laser pulse to obtain the broadest response function with high value.

Key words: terahertz, electro-optic sampling, probe laser, response function

PACS: 42.65.Re, 07.57.Hm, 42.65.Ky, 42.65.Lm

探测光波长对太赫兹波电光取样探测技术的影响

杜海伟*, 彭晓昱

(中国科学院重庆绿色智能技术研究院 太赫兹技术研究中心,重庆 400714)

摘要:由于太赫兹波电光取样探测技术中电光晶体存在的色散关系,探测光的波长会直接影响到电光取样的探测带宽和效率.由于该色散关系的存在,不同的电光晶体在电光取样中响应函数不同.本文研究了两种典型的电光晶体-碲化锌和磷化镓晶体的响应函数,发现在选取的四种探测激光波长内(600 nm、800 nm、1200 nm、1600 nm),800 nm的探测激光更合适碲化锌晶体,1200 nm的激光更合适磷化镓晶体.对于不同厚度的晶体,存在一个最优化的探测激光波长,使得该晶体的电光响应函数有最宽的带宽.

关 键 词:太赫兹波;电光取样;探测激光;响应函数

中图分类号:O434.3　　**文献标识码**:A

Introduction

Terahertz (THz) free-space electro-optic sampling (EOS) detection method has been widely used to obtain the time waveform of THz waves because of its sensitive detection of amplitude and phase since it was demonstrated more than two decades ago[1-2]. With the development of ultrafast lasers and THz technology, EOS method has shown its extensive applications such as THz time-domain spectroscopy, THz imaging, and optical pump-THz probe technology[3-5]. The EOS is based on the optical Pockels effect, in which the THz field works as a bias field to induce a birefringence in the electro-optic (EO) crystal. By collinearly or noncollinearly transmitting through the crystal with the THz pulse, an optical pulse can synchronously probe the transient index change induced by the birefringence in the crystal. A quarter-wave plate is used to make the optical pulse polarization balanceable, and a polarizer (usually a Wollaston polarizer) separates the two polarization components of the optical pulse into two beams that can be detected by two pho-

Received date: 2016-10-31, **revised date**: 2017-03-17　　**收稿日期**:2016-10-31, **修回日期**:2017-03-17

Foundation items:Supported by the Key Project of the Special Fund for Research in Basic Science and Frontier Technology in Chongqing (cstc2015jcyjBX0030) and the Innovative Research Fund (Y52A010V10) of Chongqing Institute of Green and Intelligent Technology, Chinese Academy of Sciences.

Biography:Du Hai-Wei (1980-), male, Henan Anyang, Doctor. Research areas involve optical terahertz generation, detection, and its applications.

* **Corresponding author**:E-mail:haiweidu@cigit.ac.cn

todetectors. In this scheme, the phase change of the probe optical beams induced by the THz field in the crystal through Pockels effect is transformed to the intensity variation of the probe pulse. This phase change of the optical probe pulse is proportional to the strength of THz field, thus the THz time waveform can be obtained by changing the time delay between the THz pulse and the optical probe pulse continuously[6].

The EO crystal is a key factor in the EOS detection technique. To realize the effective detection, a good phase match between the THz pulse and the probe laser pulse, and a large electro-optic coefficient for an EO crystal are desirable. Zinc-blende crystals including zinc telluride (ZnTe) and gallium phosphide (GaP)[7-8] are the typical EO crystals used in EOS technique at present. However, ZnTe and GaP show strong transverse-optical resonances at 5.3 THz[9] and 11 THz[10], respectively. These resonances bring the detection limitations around the resonance frequencies. As a result, they affect the bandwidth of the EOS detection.

The development of ultrashort laser system now can make access to high peak power femtosecond or picosecond laser pulses at different wavelengths[11], which in turn improve their applications in the extreme nonlinear optics and ultrafast optics. It is possible to generate and detect the THz pulses with laser pulses at wavelength from several hundred nm to several μm[12-14]. B. Pradarutti *et al.* have investigated the THz generation and detection with femtosecond laser pulses at 1060 nm[15]. It is necessary to know the detection efficiency, limitation and influence of probe laser in THz EOS detection. Due to the reason that both ZnTe and GaP crystals are widely used in THz EOS detection systems, in this paper, we focused on the study of the response function of these two crystals by changing of the wavelength of the probe laser from 600 nm to 1600 nm. We found that the probe laser with wavelengths of 800 nm and 1200 nm are more suitable for the ZnTe- and GaP-based EOS system in the selected four wavelengths 600 nm, 800 nm, 1200 nm, and 1600 nm, respectively. We also found that for a given thickness of an EO crystal, there exists an optimal wavelength for the probe laser pulse to obtain the broadest response function with higher value. Our results would be helpful in understanding deeply the response function of EO crystal in the EOS detection, and in rational allocation between the EO crystal thickness and the wavelength of the probe laser pulse applied in EOS detection system.

1 Theory

The index of refraction for visible and infrared light in ZnTe and GaP can be given by Ref. [16]:

$$w(\lambda) = \sqrt{A + \frac{B + \lambda^2}{\lambda^2 - C}} \quad , \quad (1)$$

in which $A = 4.27$, $B = 3.01$ and $C = 0.142$ for ZnTe, while $A = 2.680$, $B = 6.40$ and $C = 0.090\ 327\ 9$ for GaP, and λ in μm. The index calculated from Eq. (1) is agreeable with measurement data[17-18], so it can describe the index of light in the crystal. Figure 1 is the curves of refractive index of ZnTe and GaP as a function of wavelength. Although here we just give the calculated results of refractive index of ZnTe and GaP, their experimental data can be found in Refs. [17-18]. When the lasers propagate in these crystals, the refractive index of them affects the phase velocity of the lasers and the velocity match between the laser pulses and the THz pulses. From Eq. (1), the group velocity of the lasers in these crystals also can be obtained by $v_{\text{laser\_g}} = \frac{c}{n}\left(1 + \frac{\lambda}{n}\frac{dn}{d\lambda}\right)$.

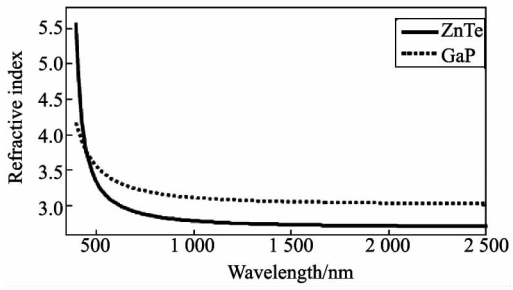

Fig. 1　Refractive index of ZnTe and GaP as a function of laser wavelength
图 1　碲化锌晶体和磷化镓晶体的折射率曲线

In the THz region, the complex dielectric function for EO crystals is given by:

$$\varepsilon(f) = \varepsilon_{\text{el}} + \frac{S_0 f_0^2}{f_0^2 - f^2 - i\Gamma_0 f} \quad , \quad (2)$$

where the first term is from the distribution of bound electrons and the second term is from the sum to the lowest transverse-optic (TO) lattice oscillation. The TO lattice oscillation is the main lattice oscillation. The parameters ε_{el}, S_0, f_0, and Γ_0 are constants used to fit to the experimental data. In calculation, $\varepsilon_{\text{el}} = 7.4$, $S_0 = 2.7$, $f_0 = 5.3$ THz, and $\Gamma_0 = 0.09$ THz for ZnTe, and $\varepsilon_{\text{el}} = 8.7$, $S_0 = 1.8$, $f_0 = 10.98$ THz, and $\Gamma_0 = 0.02$ THz for GaP[16]. After the $\varepsilon(f)$ is calculated from the Eq. (2), the complex of refraction can be obtained by taking the square root of it, $n(f) + i\kappa(f) = \varepsilon(f)^{1/2}$

When the laser pulse and the THz pulse collinearly propagate in the EO crystal, the mismatch between the phase velocity of THz pulse and the group velocity of laser pulse determines the efficiency and the bandwidth of the EOS decection. Generally, a response function is used to describe the efficiency on frequency bandwidth of EOS detection[16]. The response function of the EOS detection technique is given by Ref. [16]

$$G(f,d) = \frac{2}{1 + n(f) + i\kappa(f)} \frac{1}{d}\int_0^d\int_{-\infty}^{\infty} \exp\{[i(kz - 2\pi ft)]\delta(z - v_g f)\}\exp(-\alpha z)\,dt\,dz \quad , (3)$$

which is also dependent on the thickness of the EO crystal d. Here, the term $\frac{2}{1 + n(f) + i\kappa(f)}$ is the frequency-dependent transmission coefficient for the THz pulse from the vacuum into the EO crystal, δ function characterizes the transient feature of Pockels effect of THz field on laser pulse in the EO crystal, $\alpha = \frac{2\pi f\kappa}{c}$ is the absorption coefficient of the crystal. Equation (3) can be simplified

as follows,

$$G(f,d) = \frac{2}{1+n(f)+i\kappa(f)}\frac{1}{d}\int_0^d \exp\{[i2\pi fz(\frac{1}{v_{ph}(f)} - \frac{1}{v_{laser\_g}})]\}\exp(-\alpha z)\,dz \quad , \quad (4)$$

where $v_{ph}(f)$ is the phase velocity of THz pulse at frequency f, v_{laser_g} is the group velocity of the probe laser. The EO coefficient r_{41}, which exhibits a strong frequency dependence, is also affected by the TO lattice oscillations as the dielectric function. r_{41} is given by

$$r_{41}(f) = d_E(1+\frac{Df_0^2}{f_0^2-f^2-i\Gamma_0 f}) \quad , \quad (5)$$

where f_0 and Γ_0 are the same parameters as used in Eq. (2), and D = -0.07, $d_E = 4.25\times10^{-12}$ V/m for ZnTe, while D = -0.53, $d_E = 1\times10^{-12}$ V/m for GaP[16]. Thus, the whole response function including the EO coefficient is $G_{EOS}(f,d) = G(f,d)\cdot r_{41}(f)$.

The response function $G_{EOS}(f,d)$ describes the response of the EO crystal with different thickness and at different frequency of the probe laser pulse. This frequency also affects the bandwidth of EOS detection, thus a proper thickness for the EO crystal need to be optimized when using a probe laser at a given frequency.

2 Simulations and discussion

In order to understand how the frequency of the probe laser affects the THz EOS detection, we calculated and analyzed the response functions of typical two EO crystals, ZnTe and GaP, using the equations mentioned above. For the ultrashort laser pulses, their frequency bandwidth is usually broad up to several tens nm around a central wavelength. Here, for simplicity, the wavelength of the probe lasers denotes their central wavelengths.

First, we studied the response function of the ZnTe crystal. Figure 2 shows the curves of the response function of the ZnTe crystal at different thickness with 800 nm probe laser. One can see that when the thickness increases from 0.5 mm to 2mm, its bandwidth decreases from 3.2 THz to 2.5 THz, consistent with the previous works[10]. Thus, a thinner EO crystal is desirable in order to cover a more broadband THz radiation in the EOS detection. On the other hand, when the frequency of probe laser is changed, its group velocity changes because of the dispersion of the lasers in EO crystal. As a result, the response function alters. Figure 3 shows the response functions of ZnTe crystal with different thickness used at typical four wavelengths (a) 600 nm, (b) 800 nm, (c) 1200 nm, and (d) 1600 nm of the probe laser. The response function of 600 nm shows a flat curve in the low frequency with a small peak at around 4.3 THz, as shown in Fig. 3(a). The peak at around 4.3 THz is also generated from the phase retardation of the probe laser. When the ZnTe is very thin (~0.1 mm), this phase retardation is obvious and thus the response function here is not zero. When the ZnTe becomes thick, the velocity mismatch of the probe laser pulse and the THz pulse dominates the phase retardation, and induces a cancellation for it. As a result, there is a large dip in the response function. Among these two-dimensional figures, one may find that the optimal wavelength of the probe laser is around 800 nm for the ZnTe crystal in EOS detection due to its much broader response function than other three lasers. Thus, these results mean that the ZnTe crystal with the probe laser at around 800 nm is more suitable for application in the ZnTe-based EOS detection in these four probe lasers. From Figs. 2-3, one can observe that the detection bandwidth of EOS sensor tends to 4 THz if a thin ZnTe crystal with thickness less than 0.1mm is used. However, a very thin crystal will result in a reduction of the detection sensitivity. In practice, we may compromise between these two factors to obtain suitable detection sensitivity and bandwidth.

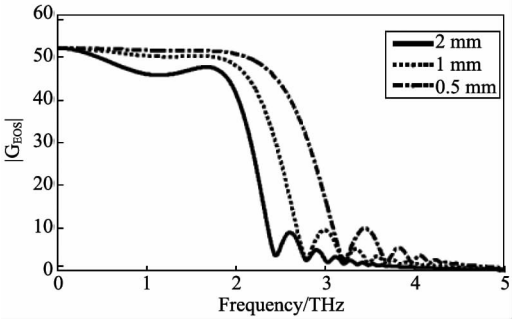

Fig. 2 Response functions of EOS when the thickness of the ZnTe crystal is 0.5 mm, 1 mm, and 2 mm, respectively

图2 不同厚度的碲化锌晶体的响应函数

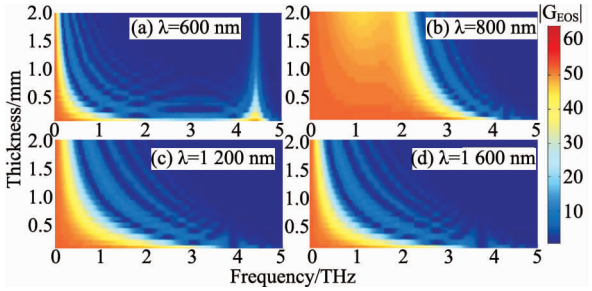

Fig. 3 Response function of ZnTe as a function of the its thickness probed by different lasers with wavelength of (a) 600 nm, (b) 800 nm, (c) 1200 nm, and (d) 1600 nm, respectively. The right color bar denotes the value of the response function

图3 不同厚度的碲化锌晶体在不同的探测光波长条件下的响应函数,(a)为600 nm,(b)为800 nm(c)为1200 nm,(d)为1600 nm. 右侧颜色条表征了响应函数的值

Second, we investigated the response functions of GaP with probe laser at different wavelengths. Here, the same four wavelengths 600 nm, 800 nm, 1200 nm and 1600 nm of the probe laser are used. The results are shown in Fig. 4. It can be seen that the response functions of EOS at 600 nm and 800 nm probe lasers have two sharp zones, one in the low frequency and the other in 9.7 THz for 600 nm, 8.3 THz for 800 nm. These sharp zones also means that the phase retardation of the probe laser in the GaP is not flat, and the reason is the

same as for ZnTe previous. These two response functions mean that it will change the waveforms of broadband THz pulses in EOS with a GaP sensor. Among these four probe lasers, it is clear that a very large range of GaP crystal thickness can be adopted if the wavelength of a probe laser is about 1200 nm in the EOS technique. This means that a laser with wavelength around 1200 nm is more suitable for applying in the GaP-based EOS detection technique. From Fig. 4(c), similar to the case of ZnTe, if one expect broader detection bandwidth of the GaP-based EOS system, a thinner crystal is desirable. One can see that the detection bandwidth tends to 8 THz if a thin GaP crystal with thickness less than 0.1 mm is applied. Although only four wavelengths were used in the calculation, the response function of other lasers can be obtained with the same method.

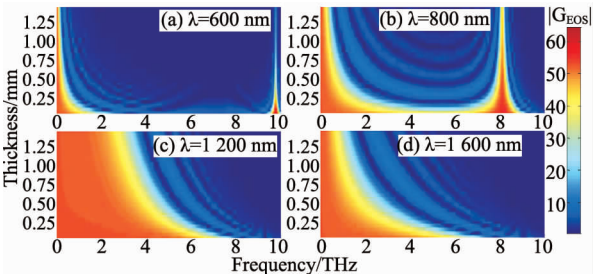

Fig. 4　Response function of GaP as a function of its thickness probed by different lasers with wavelength of (a) 600 nm, (b) 800 nm, (c) 1200 nm, and (d) 1600 nm, respectively. The right color bar denotes the value of the response function

图 4　不同厚度的磷化镓晶体在不同的探测光波长条件下的响应函数,(a)为 600 nm,(b)为 800 nm(c)为 1 200 nm,(d)为 1 600 nm

As shown in Fig. 4, the response functions for these four wavelengths are obvious different. It is necessary to investigate the evolution of the response function of GaP with the probe laser wavelength. To see how the response function evolves with the wavelength of probe laser, we set the thickness of GaP crystal at 0.5 mm and calculated the response function at different wavelength of the probe laser from 500 nm to 2000 nm. The results are shown in Fig. 5. One may find that, for a given thickness of 0.5 mm of the GaP-based EOS system, there is a best wavelength around 1 000 nm for the probe laser to obtain high value of response function and cover the broadest THz frequency band(over 6.5 THz with the response function value larger than 40). We changed the thickness of GaP crystal and recalculated the response function at different wavelengths of the probe laser. The results also show different best wavelengths. Theoretically, our results indicate that one may optimize the probe laser wavelength for the EOS system if an EO crystal style and its thickness are given. In practice, this would be meaningful to the option of the possible probe laser with the suitable wavelength for the EOS detection system.

3　Conclusion

In conclusion, we studied the response functions of two typical EO crystals, ZnTe and GaP, based THz EOS

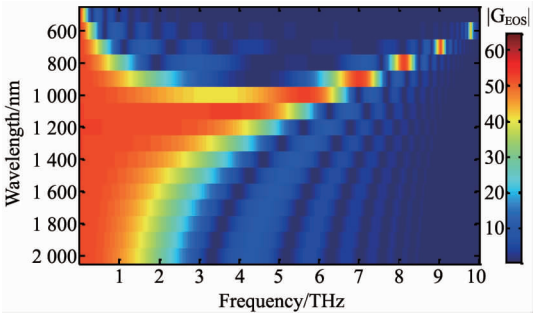

Fig. 5　The evolution of response function of 0.5 mm thick GaP with the change of probe laser wavelength. The right color bar denotes the value of the response function

图 5　0.5 mm 厚的磷化镓晶体的响应函数随探测光波长变化的演化

detection method. The response function reflects the capability of the detection efficiency and the detection bandwidth of the EOS system. Thus, the detail of calculation of response function is given. Our numerical results indicate that the probe laser with wavelengths of 800 nm and 1200 nm are more suitable for the ZnTe and GaP-based THz EOS system, respectively, than other three selected wavelengths. We also found that for a given thickness of an EO crystal, there exists an optimal wavelength for the probe laser pulse to obtain the broadest response function with high value. For a given probe laser, a thinner EO crystal is desirable for broader detection bandwidth of the EOS system at the expense of the sensitivity of the EO crystal.

References

[1] Wu Q, Zhang X C. Free-space electro-optic sampling of terahertz beams [J]. 1995 *Applied Physics Letters*, 1995, **67**(24): 3523-3525.

[2] Nahata A, Weling A S, Heinz T. A wideband coherent terahertz spectroscopy system using optical rectification and electro-optic sampling [J]. *Applied Physics Letters*, 1996, **69**(16): 2321-2323.

[3] Kampfrath T, Tanaka K, Nelson K. Resonant and nonresonant control over matter and light by intense terahertz transients [J]. 2013 *Nature Photonics*, 2013, **7**: 680-690.

[4] Zouaghi W, Thomson M D, Rabia K, *et al*. Broadband terahertz spectroscopy: principles, fundamental research and potential for industrial applications [J]. *European Journal of Physics*, 2013, **34**: S179-S199.

[5] Ulbricht R, Hendry E, Shan J, *et al*. Carrier dynamics in semiconductors studied with time-resolved terahertz spectroscopy [J]. *Reviews of Modern Physics*, 2011, **83**(2): 543-586.

[6] Chen Q, Tani M, Jiang Z, *et al*. Electro-optic transceivers for terahertz-wave applications [J]. *Journal of Optical Society of America B*, 2001, **18**(6): 823-831.

[7] Wu Q, Zhang X C. Ultrafast electro-optic field sensors [J]. *Applied Physics Letters*, 1996, **68**(12): 1604-1606.

[8] Wu Q, Zhang X C. 7 terahertz broadband GaP electro-optic sensor [J]. *Applied Physics Letters*, 1997, **70**(14): 1784-1786.

[9] Gallot G, Zhang J, Mcgowan R W, *et al*. Measurements of the THz absorption and dispersion of ZnTe and their relevance to the electro-optic detection of THz radiation [J]. *Applied Physics Letters*, 1999, **74**(23): 3450-3452.

(下转第 294 页)

characteristics of dark current for arsenic doped LWIR HgCdTe detectors [J]. *Infra. Phys. Technol.* 2013, **61**: 157－161.
[7] NGUYEN T, MUSCA C A, Dell J M, *et al*. Dark currents in long wavelength infrared HgCdTe gated photodiodes [J]. *J. Electronic Mat*. 2004. **33**(6):621－629.
[8] Gopal V, Xie X, Liao Q, *et al*. Analytical modelling of carrier transport mechanisms in long wavelength planar n + － p HgCdTe photovoltaic detectors [J], *Infra. Phys. Technol.* 2014, **64**:56－61.
[9] Gopal V, Li Q, He j, *et al*. Current transport mechanisms in mercury cadmium telluride diode [J], *J. Appl. Phys*, 2016, **120**:084508.
[10] Hu W, Chen X, Y, *et al*. Analysis of temperature dependence of dark current mechanisms for long-wavelength HgCdTe photovoltaic infrared detectors [J]. *J. Appl. Phys*. 2009, **105**(104502): 1－8.
[11] Bai Y, Qiao H, Li X, *et al*. Effects of annealing on HgCdTe detectors after γ irradiation [J]. *High Power Laser and particle Beam*. 2007, **02**:301－304.
[12] Gopal V, Gupta S, Bhan R K, *et al*. Modeling of dark characteristics of mercury cadmium telluride n^+-p junctions [J]. *Infra. Phys. Technol*. 2003. **44**:143－152.
[13] Nemirovskyy, Rosenfeld D, Adar R, *et al*. Tunneling and dark currents in HgCdTe photodiodes [J]. *J. Vac. Sci. Technol*. 1989. A**7**:528－535.
[14] Martyniuk P, Rogalski ,A. MWIR barrier detectors versus HgCdTe photodiodes [J], *Infra. Phys. Technol.* 2015, **70**:125－128.
[15] Qiu W. ,Hu W. ,Lin C. ,*et al*. Surface Leakage Current in 12.5μm Long-wavelength HgCdTe Infrared Photodiode Arrays [J]. *Optics Letters*. 1989. **41**:828－831.
[16] Reine M B, Sood A K, Tredwell T J. Mercury cadmium telluride photovoltaic infrared detectors [M]. New York; Academic Press. 1981: 216－220.
[17] Rogalski A. Infrared detectors [M]. 2nd ed. Boca Raton, Florida: CRC Press. 2011:206－208.
[18] Blanks D K, Beck J D, Kinch M A, *et al*. Band-to-band tunnel processes in HgCdTe: Comparison of experimental and theoretical studies [J]. *J. Vac. Sci. Technol*. 1988. A**6**: 2790－2794.
[19] Singh S K, Gopal V, Mehra R M. Relationship between deep levels and R_0A product in HgCdTe diodes [J]. *Opto-Electro. Rev*, 2001. **9**(4):385－390.
[20] Gopal V, Singh S K, Mehra R M. Analysis of dark current contributions in mercury cadmium telluride junction diodes [J]. *Infra. Phys. Technol*. 2002. **43**:317－326.
[21] Gopal V, Gupta S, Bhan R K, *et al*. Modeling of dark characteristics of mercury cadmium telluride n^+-p junctions [J]. *Infra. Phys. Technol*. 2003. **44**:143－152.
[22] Gopal V, Qiu W, Hu W, Modelling of illuminated current － voltage characteristics to evaluate leakage currents in long wavelength infrared mercury cadmium telluride photovoltaic detectors [J], *Journal of Applied Physics*. 2014, **116**:184503.
[23] Quan Z, Li Z, Hu W, *et al*. Parameter determination from resistance-voltage curve for long-wavelength HgCdTe photodiode [J]. *J. Appl. Phys*. 2006. **100**:084503.
[24] Lu W, Tao F, Mu Y, *et al*. The application of solid crystallization process in optimization algorithm [J]. *Chinese Journal of Computational Physics*. 1999, **16**:141－144.
[25] Cao J. *The effect of irradiation on semiconductor or material* [M]. Beijing: Science Press. 1993.
[26] He L, Yang D, Ni G, *et al*. *Introduction to advanced focal plane arrays* [M]. Beijing: National Defence Industry Press. 2011.
[27] Qiu W, Hu W, Lin T, *et al*. Temperature-sensitive junction transformations for mid-wavelength HgCdTe photovoltaic infrared detector arrays by laser beam induced current microscope [J]. *Applied Physics Letters*. 2014. **105**: 191106.

(上接第269页)

[10] Leitenstorfer A, Hhnsche S, Shan J, *et al*. Detectors and sources for ultrabroadband electro-optic sampling: experiment and theory [J]. *Applied Physics Letters*, 1999, **74**(11): 1516－1518.
[11] Fattahi H, Barros H, Gorjan M, *et al*. Third-generation femtosecond technology [J]. *Optica*, 2014, **1**(1): 45－63.
[12] Clerici M, Peccianti M, Schmidt B, *et al*. Wavelength scaling of terahertz generation by gas ionization [J]. *Physical Review Letters*, 2013, **110**(25): 253901.
[13] Vicario C, Monoszlai B, Jazbinsek M, *et al*. Intense, carrier frequency and bandwidth tunable quasi single-cycle pulses from an organic emitter covering the terahertz frequency gap [J]. *Scientific Reports*, 2015, **5**: 14394.
[14] Du H W, Yang N. Theoretical investigation on THz generation from optical rectification with tilted-pulse-front excitation [J]. *Chinese Physics Letters*, 2014, **31**(12):124201.
[15] Pradarutti B, Matthaus G, Bruckner C, *et al*. Electrooptical sampling of ultra-short THz pulses by fs-laser pulses at 1060 nm [J]. *Applied Physics B*, 2006, **85**:59－62.
[16] Casabuoni S, Schlarb H, Schmidt B, *et al*. Numerical studies on the electro-optic detection of femtosecond electron bunches [J]. *Physical Review Special Topics-Accelerators and Beams*, 2008, **11**(7):072802.
[17] Sliker T, Jost J. Linear electro-optic effect and refractive indices of cubic ZnTe [J]. *Journal of Optical Society of America B*, 1966, **56**: 130－131.
[18] Nelson D, Turner E. Electro-optic and piezoelectric coefficient and refractive index of gallium phosphide[J]. *Journal of Applied Physics*, 1968, **39**(7): 3337－3344.